Defective ribosome assembly in Shwachman-Diamond syndrome

Chi C. Wong,[1,2] David Traynor,[1] Nicolas Basse,[1,2] Robert R. Kay,[1] and Alan J. Warren[1,2]

[1]Medical Research Council Laboratory of Molecular Biology, Cambridge, United Kingdom; and [2]The Department of Haematology, University of Cambridge, Cambridge, United Kingdom

Shwachman-Diamond syndrome (SDS), a recessive leukemia predisposition disorder characterized by bone marrow failure, exocrine pancreatic insufficiency, skeletal abnormalities and poor growth, is caused by mutations in the highly conserved *SBDS* gene. Here, we test the hypothesis that defective ribosome biogenesis underlies the pathogenesis of SDS. We create conditional mutants in the essential *SBDS* ortholog of the ancient eukaryote *Dictyostelium discoideum* using temperature-sensitive, self-splicing inteins, showing that mutant cells fail to grow at the restrictive temperature because ribosomal subunit joining is markedly impaired. Remarkably, wild type human SBDS complements the growth and ribosome assembly defects in mutant *Dictyostelium* cells, but disease-associated human SBDS variants are defective. SBDS directly interacts with the GTPase elongation factor-like 1 (EFL1) on nascent 60S subunits in vivo and together they catalyze eviction of the ribosome antiassociation factor eukaryotic initiation factor 6 (eIF6), a prerequisite for the translational activation of ribosomes. Importantly, lymphoblasts from SDS patients harbor a striking defect in ribosomal subunit joining whose magnitude is inversely proportional to the level of SBDS protein. These findings in *Dictyostelium* and SDS patient cells provide compelling support for the hypothesis that SDS is a ribosomopathy caused by corruption of an essential cytoplasmic step in 60S subunit maturation. (*Blood*. 2011;118(16):4305-4312)

Introduction

Shwachman-Diamond syndrome (SDS; OMIM 260400), caused by recessive mutations in the *SBDS* gene,[1] has a complex phenotype that includes bone marrow failure with striking predisposition to leukemia, poor growth, exocrine pancreatic insufficiency, and skeletal abnormalities.[2] Targeted deletion of the *Sbds* gene in mice is embryonic lethal by E6.5.[3] Furthermore, homozygosity for *SBDS* null alleles has not been reported, suggesting that human *SBDS* is essential and that SDS patients carry at least one hypomorphic *SBDS* allele. Consistent with a fundamental role in cell physiology, the *SBDS* gene encodes a highly conserved protein with orthologs in archaea, plants, and all eukaryotes. X-ray crystallographic and solution NMR studies have revealed that the SBDS protein has a 3-domain architecture that is conserved from archaea to human, comprising an N-terminal FYSH (Fungal, Yhr087w, Shwachman) domain, a central 3 helical bundle and a C-terminal domain with a ferredoxin-like fold.[4-7] At the cellular level in mammalian cells, diverse functions for SBDS have been proposed, including roles in chemotaxis,[8,9] mitosis,[10] and cellular stress responses.[11] Although multiple interaction partners for the SBDS protein have been suggested,[11,12] the functional relevance of these remains unclear and none of the proposed functions immediately suggests what the specific biochemical function of the SBDS protein might be.

By contrast, genetic studies in *S cerevisiae* and mammalian cells indicate an alternate function for SBDS; namely in ribosome biogenesis.[7,13] During the final stages of cytoplasmic ribosome assembly, key factors are released from precursor 60S (pre-60S) ribosomal subunits and shuttled back to the nucleus to engage in additional rounds of 60S subunit maturation. In particular, eIF6 (yeast Tif6) is required for the biogenesis and nuclear export of pre-60S subunits.[14] The binding site for eIF6 localizes to the intersubunit interface,[15] explaining the role of eIF6 as a ribosome antiassociation factor. Hence, removal of eIF6 from nascent 60S subunits is a prerequisite for the assembly of actively translating 80S ribosomes.

The yeast SBDS ortholog, Sdo1, functions in a pathway containing the GTPase, Efl1, to facilitate the release and recycling of Tif6 from nascent cytoplasmic 60S ribosomal subunits.[13] When the *SDO1* gene is deleted in yeast, growth is severely impaired and Tif6 is mislocalized to the cytoplasm, giving a phenotype identical to cells deleted for *EFL1*.[16,17] Both the *SDO1* and the *EFL1* deletion phenotypes are suppressed by gain-of-function *TIF6* alleles encoding Tif6 mutants that may be more easily dissociated from 60S ribosomal subunits than the wild type protein.[13,16,17] Furthermore, recent genetic and biochemical data indicate that in mammalian cells, human SBDS cocatalyzes the release of eIF6 from nascent cytoplasmic 60S subunits in concert with the GTPase EFL1.[7]

However, the concept of SDS as a ribosomopathy remains controversial.[18] Thus far, studies using primary human fibroblasts from SDS patients have failed to demonstrate a defect in ribosomal subunit joining,[12] and in the absence of a robust in vivo genetic complementation assay it has not been possible to address the functional consequences of disease-associated human SBDS mutations. *Dictyostelium discoideum*, an amoebozoan, belongs to a completely different branch of the eukaryotic tree from yeast, and in evolutionary terms is approximately as far from yeast as it is from humans; *Dictyostelium* therefore represents an excellent organism in which to test the generality of the proposal that SBDS

Submitted June 2, 2011; accepted July 8, 2011. Prepublished online as *Blood* First Edition paper, July 29, 2011; DOI 10.1182/blood-2011-06-353938.

An Inside *Blood* analysis of this article appears at the front of this issue.

The online version of this article contains a data supplement.

The publication costs of this article were defrayed in part by page charge payment. Therefore, and solely to indicate this fact, this article is hereby marked "advertisement" in accordance with 18 USC section 1734.

functions in 60S ribosomal subunit maturation. In addition, *Dictyostelium* cells are strongly chemotactic, allowing for a separate test of the proposed role of SBDS in chemotaxis. We found that the *SBDS* gene in *Dictyostelium* (*sbdS*) is essential and therefore introduced a new technology to this organism to engineer conditional mutants. This method, based on the insertion of temperature-sensitive, self-splicing inteins into the genomic *sbdS* coding sequence by homologous recombination, allows rapid depletion of functional protein from cells at the restrictive temperature. We show, using these intein mutants, that *sbdS* is required for ribosomal subunit joining in *Dictyostelium* and that human *SBDS* genetically complements the *Dictyostelium* mutant. We delineate a mechanism in which SBDS and the GTPase EFL1 directly catalyze GTP-dependent eIF6 release through a direct physical interaction on the 60S ribosomal subunit. Extending this work to human cells supports the hypothesis that the role of SBDS in ribosome maturation is universal, and underlies the disease phenotype.

Methods

Strains and plasmids

The plasmids generated in this study are listed in supplemental Table 1 (available on the *Blood* Web site; see the Supplemental Materials link at the top of the online article). The *Dictyostelium* strains are listed in supplemental Table 2 and the primers used are listed in supplemental Table 3.

Dictyostelium culture

Dictyostelium cells were grown axenically[19] using HL5 plus glucose from Formedia, in 10 cm plastic Petri dishes or in shaking suspension at 22°C or 27°C. Cells were also maintained on bacterial *Klebsiella aerogenes* lawns on SM agar plates.[20] For development assays, cells were washed in KK2 buffer (16.5mM KH_2PO_4, 3.9mM K_2HPO_4, and 2mM $MgSO_4$) with 0.1mM $CaCl_2$ and plated onto 1.8% (wt/vol) nonnutrient agar plates at 22°C or 27°C.

Lymphoblastoid cell lines

Human lymphoblastoid cell lines were grown in RPMI 1640 + GlutaMAX (Gibco) with 15% FBS (PAA), penicillin, and streptomycin antibiotics.

Dictyostelium transformation

The generation of replacement constructs and expression plasmids is described in the supplemental Methods. Log phase *Dictyostelium* cells growing in axenic medium were electroporated with 10-20 μg DNA per 10^7 cells as previously described[21] and single clones selected by plating onto *K aerogenes* lawns. Correctly targeted clones were identified by PCR and immunoblotting. To normalize signals from human SBDS variants, ratios of each human SBDS-myc signal to GFP and actin were calculated. The ratio calculated for wild-type human SBDS-myc was designated as 100%.

Subcellular fractionation

Vegetative cells in mid-log phase were harvested, washed in KK2 buffer and resuspended at 2×10^7 cells/mL. One milliliter of cells was pelleted by centrifugation and lyzed in NLB buffer, which is made up of 50mM Tris-HCl pH 7.4, 5mM $(CH_3COO)_2Mg$, 10% (wt/vol) sucrose, 2% (vol/vol) NP-40 and EDTA-free protease inhibitors (Roche) by vortexing for 1 minute. Nuclei were pelleted by centrifugation at 2300*g* for 5 minutes at 4°C and the supernatant saved as the "crude cytoplasmic" fraction. The nuclear pellet, washed once in 1 mL of NLB and resuspended in 100 μL of NLB, was designated the "nuclear fraction."

Sucrose density gradients

Exponentially growing *Dictyostelium* cells were treated with cycloheximide (100 μg/mL) for 5 minutes before harvesting by centrifugation. Cells were washed once in KK2 buffer with 100 μg/mL cycloheximide and lyzed by vortexing for 1 minute in lysis buffer [50mM HEPES pH 7.5, 40mM $(CH_3COO)_2Mg$, 25 mM KCl, 5% (wt/vol) sucrose, 0.4% (vol/vol) NP-40, 100 μg/mL cycloheximide, EDTA-free protease inhibitors (Roche), and 1mM PMSF] at 2×10^8 cells/mL. The lyzate was cleared by centrifugation (8000*g* for 5 minutes at 4°C) and 10 A_{254nm} units loaded onto a 10%-50% (wt/vol) sucrose gradient in 50mM HEPES pH 7.5, 40mM $(CH_3COO)_2Mg$, 25mM KCl and EDTA-free protease inhibitors (Roche) in Polyallomer 14×95 mm centrifuge tubes (Beckman). After centrifugation (Beckman SW40Ti rotor) at 260 900*g* for 3 hours at 4°C, gradients were fractionated at 4°C using a Gilson Minipuls 3 peristaltic pump with continuous monitoring (A_{254nm}) and polysome profiles recorded using a Gilson N2 data recorder. Proteins were precipitated from 0.5 mL fractions using 20% (vol/vol) trichloroacetic acid, separated on sodium dodecyl sulfate–PAGE gels and transferred to nitrocellulose membranes for immunoblotting. For ribosome profiles, $(CH_3COO)_2Mg$ and cycloheximide were removed from all buffers. Five A_{254nm} units of *Dictyostelium* cell lysates were loaded onto 10%-50% (wt/vol) sucrose gradients and centrifuged at 260 900*g* for 4 hours at 4°C.

For human lymphoblastoid cell polysome profiles, cells were grown to $\sim 0.6 \times 10^6$ cells/mL, treated with cycloheximide (100 μg/mL) for 15 minutes, washed in ice-cold PBS and stored at −80°C. Cells were lysed in buffer A, which is made up of 20mM HEPES pH 7.5, 50mM KCl, 10mM $(CH_3COO)_2Mg$, EDTA-free protease inhibitors (Roche), supplemented with cycloheximide 100 μg/mL, 1mM PMSF, 100 U/mL RNase inhibitor (Promega), 1% (vol/vol) sodium deoxycholate, and 0.4% (vol/vol) NP-40 at 10^8 cells/mL for 10 minutes on ice. Lysates were cleared by centrifugation before sedimentation through 10%-50% sucrose gradients in buffer A.

Purification of *Dictyostelium* 60S ribosomal subunits

60S ribosome fractions were collected from 6×38 mL polysome profile gradients as described in "Sucrose density gradients" using 2×750 mL cultures of cycloheximide-treated $sbdS^{int(ts)}$ cell cultures grown for 12 hours at 27°C. 60S ribosome fractions were collected from 10%-35% (wt/vol) sucrose gradients prepared in ribosome buffer B, made up of 50mM HEPES pH 7.5, 200mM KCl, 10mM $(CH_3COO)_2$ Mg, 2mM DTT, by centrifugation (SW32 rotor) at 174 900*g* for 5.5 hours at 4°C. Fractions were pooled, diluted 2-fold in ribosome storage buffer C, made up of 20mM HEPES pH 7.5, 100mM KCl, 5mM $(CH_3COO)_2$ Mg, 2mM DTT, 250mM sucrose, and pelleted by centrifugation (SW70Ti rotor) at 208 430*g* for 18 hours at 4°C, before resuspension in storage buffer C to $\sim$ 100 A_{254nm} U/mL.

eIF6 release assay

Recombinant human SBDS and EFL1 proteins were expressed in *E coli* and yeast, respectively and purified as described.[7] The reaction mixture (50 μL) contained 16 pmol purified 60S subunits, 80 pmol human SBDS or EFL1 proteins in buffer C containing 150 μM GTP, GDP, or GDPNP (Sigma-Aldrich). Reaction mixtures were incubated for 30 minutes at RT, layered onto 50 μL 15% (wt/vol) sucrose cushions in buffer C (with 150μM guanine nucleotide), and centrifuged (TLA100 rotor) at 352 900*g* for 13 minutes at 4°C. Twenty microliters of supernatant ("free") was removed, the lower 60 μL discarded and the ribosome pellet ("bound") resuspended in the residual 20 μL buffer.

Antibodies and immunoblotting

Rabbit polyclonal antibodies were raised against full-length *Dictyostelium* SBDS and affinity purified. Anti–human SBDS and EFL1 antibodies are described.[7] Additional antibodies used for immunoblotting were anti-actin (C-11; Santa Cruz Biotechnology, 1:2000), anti-eIF6 (ab37598, Abcam, 1:5000), anti-FLAG (Abcam, ab1162, 1:1000; M2, Sigma-Aldrich, 1:1000), anti-myc (R950-25, Invitrogen, 1:1000), anti-GFP (ab6673, Abcam, 1:2000; 11814460001, Roche, 1:5000), anti-RPL8 (ARP40215, Aviva Systems

Biology, 1:1000), anti-RPL23 (16 086-1-AP, Proteintech, 1:1000), anti-RPL11 (16 277-1-AP, Proteintech, 1:1000), anti-NMD3 (16 060-1-AP, Proteintech, 1:1000), anti-EBP1 (ab33613, Abcam, 1:5000) and anti-histone H3 (ab1791, Abcam, 1:2000). HRP-conjugated secondary antibodies were obtained from GE Healthcare and Abcam.

For immunoblotting, *Dictyostelium* cells were lysed directly in SDS sample buffer. Human lymphoblastoid cells were lyzed in CelLytic M (Sigma-Aldrich) supplemented with protease inhibitors and protein concentrations determined by Bradford assay. Densitometry analysis was performed using ImageJ 1.42q (National Institutes of Health).

Immunoprecipitation assays

Log-phase cells were washed twice in PBS and resuspended to 5×10^7 cells/mL in lysis buffer (PBS, EDTA-free protease inhibitors [Roche], 1mM PMSF, and 1mM Na_3V0_4). DSP or DSS cross-linking reagents (Pierce) were added to 1mM to 1 mL of cells for 20 minutes at room temperature. Tris-HCl (pH 7.4) was added to 100mM for 20 minutes to quench the crosslinking reaction. Triton X-100 was added to 1% (vol/vol) and the lyzates rotated for 4 hours at 4°C. After clearing by centrifugation, the sample supernatant was incubated with the immunoprecipitation antibody for 1 hour before adding protein A beads (Sigma-Aldrich) or anti-FLAG M2 agarose (Sigma-Aldrich) overnight. RNase (10 μg/mL) was added to lysates for 30 minutes. After 4 washes in lysis buffer, the beads were boiled in reducing sodium dodecyl sulfate sample buffer containing 0.7M β-mercaptoethanol before immunoblotting.

Mass spectrometry

Protein samples were resolved by sodium dodecyl sulfate–PAGE and stained with Coomassie blue. Gel bands were reduced and alkylated before overnight digest with porcine Trypsin (Promega). Peptides were extracted from gel bands and separated on an Ultimate 3000 HPLC system with a 15 cm × 75 μm i.d. Acclaim PepMap C18 column (Dionex) and analyzed on a LTQ XL Orbitrap mass spectrometer (Thermo Scientific). Protein identification was carried out using an in-house Mascot NCBI database.

Chemotaxis assays

Aggregation-competent cells were prepared for chemotaxis assays as previously described.[21] *Dictyostelium* cells were placed at opposite ends of a Dunn chamber with 1 μm cAMP chemoattractant in the central reservoir. For experiments performed at the nonpermissive temperature, cells were pre-incubated at 27°C for 1 hour and the stage incubator was maintained at 27°C during chemotaxis recordings. DIC images were captured every 20 seconds for 20 minutes. Chemotaxis parameters were calculated from movies recorded from 3 independent experiments using Manual Tracking and Chemotaxis Tool plugins in ImageJ Version 1.37 (National Institutes of Health).

Results

SBDS inactivation using conditional splicing inteins in *Dictyostelium*

To devise a genetic strategy to manipulate SBDS function in *Dictyostelium,* we first tested whether the gene, *sbdS*, (DDBG0272324; http://dictybase.org/) is essential. The endogenous gene can readily be targeted by homologous recombination, but we found it impossible either to knock out, or to knock a stop codon into the coding sequence, demonstrating that the gene itself is essential (supplemental Figure 1). We therefore introduced a technology to engineer conditional mutants in *Dictyostelium*, based on a temperature-sensitive intein, which is introduced into the endogenous gene of interest by homologous recombination, and is able to splice itself out to create a functional protein at the permissive but not at the restrictive temperature[22] (Figure 1A).

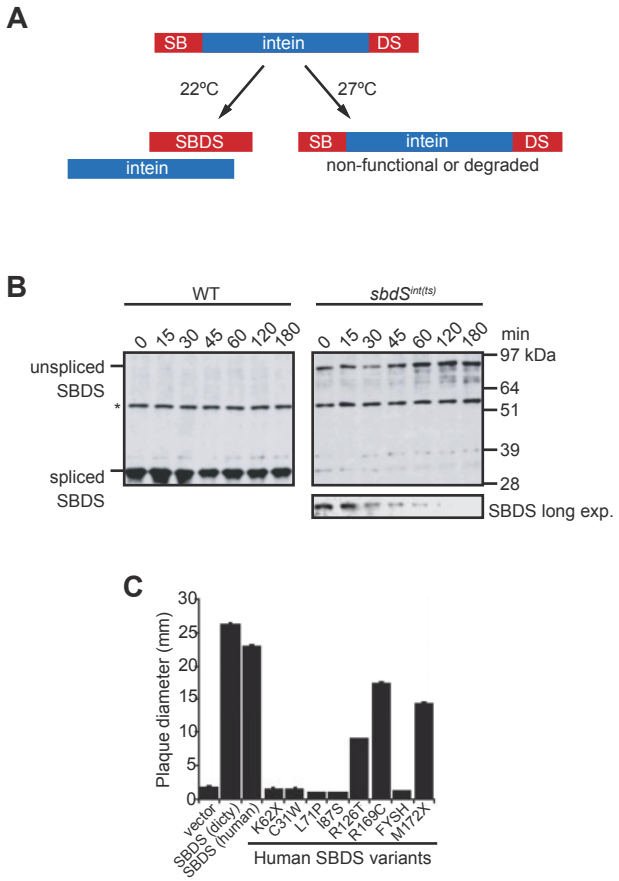

Figure 1. Human and *Dictyostelium* SBDS are functional orthologs. (A) Schematic representation of the temperature-dependent intein splicing system to conditionally inactivate the *Dictyostelium* SBDS protein. (B) Temperature-dependent depletion of *Dictyostelium* SBDS protein in vivo. Spliced and unspliced SBDS proteins were detected by immunoblotting of wild type (WT) and *sbdS*$^{int(ts)}$ cell extracts at the nonpermissive temperature (27°C). *Indicates nonspecific band used as loading control. (C) Plaque assays of *sbdS*$^{int(ts)}$ cells transfected with empty vector control (pDM317) or plasmids expressing *Dictyostelium* SBDS or the indicated human SBDS-myc variants. Mean size of 10 plaques ± SEM at 7 days at 22°C is presented.

As a first step, targeted replacement of the endogenous wild type *sbdS* gene with an allele encoding an SBDS protein containing a wild type (nontemperature-sensitive, *sbdS*$^{int(WT)}$) version of the intein, produced fully functional SBDS protein and the cells had no obvious phenotype (supplemental Figure 2A-F). By contrast, cells expressing the temperature-sensitive version of SBDS (*sbdS*$^{int(ts)}$) also grew nearly normally at the permissive temperature (22°C) in axenic medium (doubling time of 14 hours compared with 12 hours for controls), but were impaired when grown on bacteria, where the faster growth rate of *Dictyostelium* cells poses a much greater demand on protein synthesis (supplemental Figure 3A-C).

By contrast, compared with wild type controls, cells carrying the temperature-sensitive *sbdS*$^{int(ts)}$ allele completely failed to grow at the restrictive temperature (27°C) either axenically (supplemental Figure 3D) or on bacteria (data not shown). SBDS protein was expressed at considerably lower levels in *sbdS*$^{int(ts)}$ cells, even at the permissive temperature (though obviously sufficient to support growth), but was barely detectable by immunoblotting within 2 hours of incubation at the restrictive temperature (Figure 1B).

As *Dictyostelium* cells are strongly chemotactic to cAMP during the aggregation stage of their developmental program (around 4-8 hours of starvation), we could therefore test whether chemotaxis depends on SBDS function. We found that chemotaxis was unimpaired in temperature-sensitive *sbdS*$^{int(ts)}$ cells that had

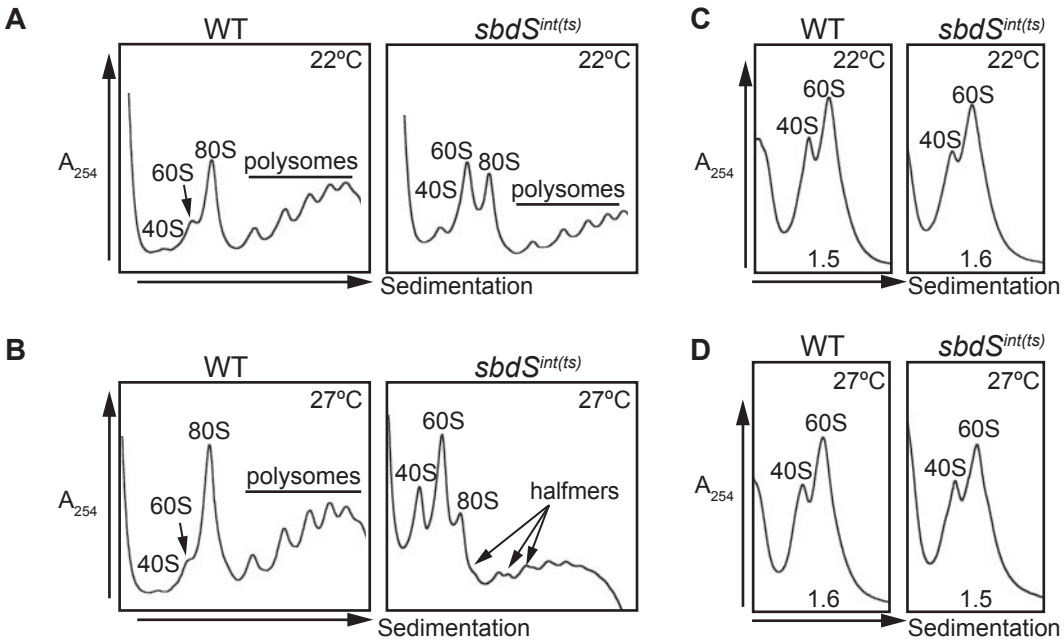

Figure 2. SBDS is required for ribosomal subunit joining in *Dictyostelium*. (A-B) Subunit joining defect in SBDS-depleted (*sbdS*$^{int(ts)}$) cells. Polysome profiles of extracts from *sbdS*$^{int(ts)}$ compared with wild type cells cultured at (A) the permissive (22°C) or (B) the restrictive (27°C) temperature. Arrows indicate halfmer polysomes. (C-D) SBDS depletion does not alter the ratio of 60S to 40S subunits. Ribosome profiles of extracts from *sbdS*$^{int(ts)}$ compared with wild type cells cultured at (C) 22°C and (D) 27°C. The 60S:40S subunit ratios are indicated.

been pre-incubated for one hour at the restrictive temperature (supplemental Figure 4), arguing strongly against a direct role of SBDS in chemotaxis. However, later stages of multicellular development of these cells were delayed, and they arrested approximately half way through the program as loose mounds (roughly 12 hours of starvation; supplemental Figure 5) at a time when synthesis of a large block of developmental proteins is normally up-regulated.[23]

Human SBDS complements the ribosome assembly defect in mutant *Dictyostelium* cells

We next used the conditional SBDS mutant in a genetic test of the evolutionary conservation of SBDS function. As expected, the growth and developmental defects in SBDS-depleted *Dictyostelium* cells could be complemented by ectopically expressing the *Dictyostelium* SBDS protein (Figure 1C and supplemental Figure 6). More remarkably, the human *SBDS* gene also complements the growth and developmental defects (Figure 1C and supplemental Figure 6). *SBDS* genes carrying SDS-associated mutations complemented less well than wild type, and with the exception of SBDS^{R126T}, which appears to be functionally impaired, their effectiveness correlated with the level of protein expressed, as assessed by immunoblotting (Figure 1C and supplemental Figure 7A-C). While the M172X truncation mutant (domains I and II) complements, the N-terminal FYSH domain alone does not, indicating that the C-terminal domain is not critical for SBDS function in vivo. Complementation across such a wide evolutionary distance strongly argues that the basic function of SBDS must also be evolutionarily conserved.

We next examined the SBDS-depleted cells for a defect in ribosomal subunit joining. Using sucrose density gradients, we found that even at the permissive temperature, compared with wild type cells, *sbdS*$^{int(ts)}$ cells have increased levels of free 40S and 60S subunits and decreased levels of mature 80S ribosomes (Figure 2A). Incubation of *sbdS*$^{int(ts)}$ cells at 27°C for 12 hours dramatically exacerbated the defect, with the appearance of halfmer polysomes (representing 40S ribosomes on mRNA lacking 60S subunits; Figure 2B). By contrast, there was no difference in the ratio of 60S to 40S subunits in *sbdS*$^{int(ts)}$ cells, compared with wild type, either at 22°C or 27°C (Figure 2C-D). As controls, we found that polysome profiles were normal in *sbdS*$^{int(WT)}$ cells grown at 22°C and 27°C, indicating that the intein itself is not responsible for the defect in ribosome assembly and that ectopically expressed *Dictyostelium* SBDS protein corrected the polysome profiles, showing that the effects are not because of a dominant negative effect of the mutant protein (supplemental Figure 8A-C). The human *SBDS* gene, but not SDS-associated disease mutants, complemented the defect in ribosomal subunit joining (supplemental Figure 7D). Taken together, these data indicate that SBDS has a conserved function in ribosomal subunit joining.

We next tested for an interaction between the genes encoding SBDS (*sbdS*) and eIF6 (*eifF*, DDBG0276493). First, we found that if eIF6 is overexpressed in wild type cells, it impairs ribosomal subunit joining, thus mimicking the effect of SBDS deficiency (supplemental Figure 9A-C). Second, and more significantly, the ribosomal subunit joining defect in *sbdS*$^{int(ts)}$ cells, as well as their growth and developmental phenotypes, can be suppressed by expressing a mutant form of eIF6 with reduced affinity for 60S ribosomal subunits (Figure 3A-D and supplemental Figures 6,10), confirming a genetic interaction between *sbdS* and *eifF*.

In wild type cells, eIF6 binds pre-60S subunits in the nucleus and is exported with them into the cytoplasm, where it is released. Reflecting this cycling behavior, eIF6 is found in both nuclear and cytoplasmic compartments. By comparison with wild type, the proportion of eIF6 in the cytoplasm increases in SBDS-depleted *Dictyostelium* cells (Figure 3E-F), and it predominantly cosediments with pre-60S subunits in high salt conditions that favor eIF6 dissociation from pre-60S subunits in wild type cells (Figure 3G). Furthermore, we found by chance that SBDS-GFP, but not GFP alone, acts as a dominant negative protein whose expression results

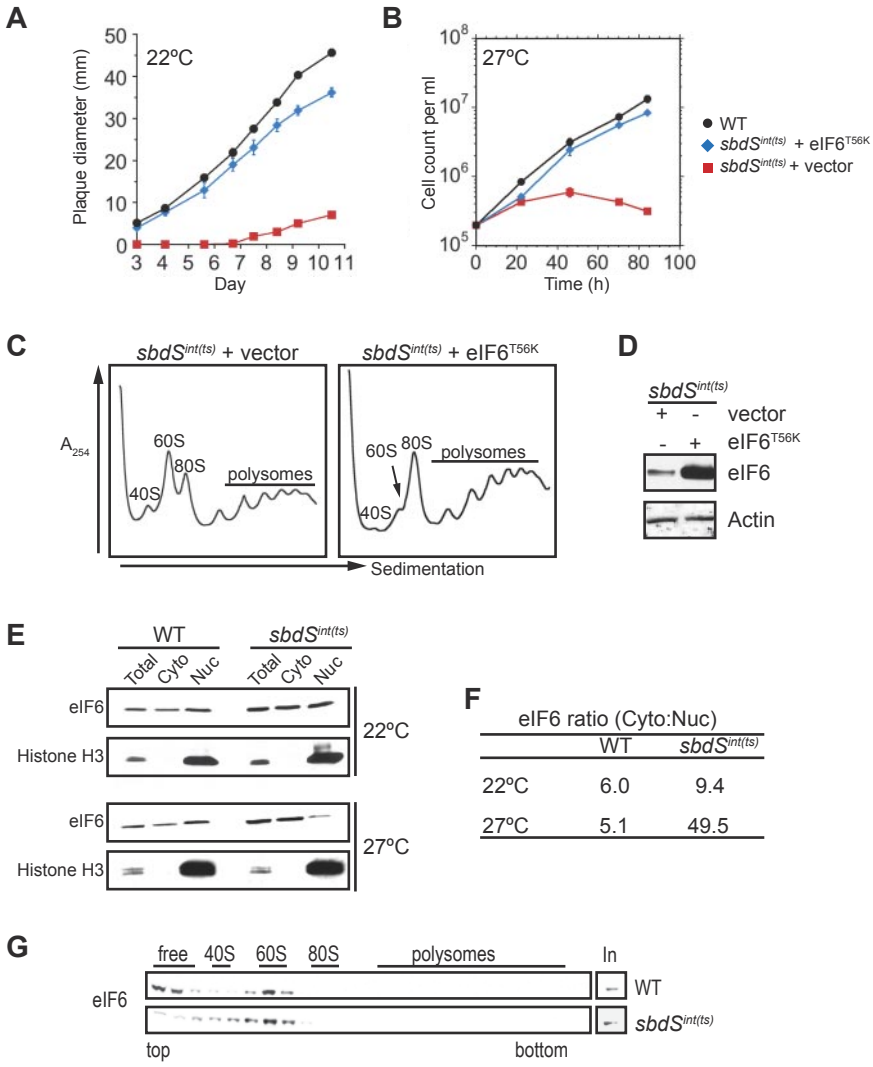

Figure 3. Gain-of-function eIF6 mutant bypasses the requirement for SBDS in *Dictyostelium*. (A-B) eIF6^{T56K} suppressor rescues the growth defect of SBDS-depleted cells. Growth of *sbdS*$^{int(ts)}$ cells transformed with empty vector control (red squares) or a plasmid expressing eIF6^{T56K} (blue diamonds) compared with wild-type (black circles; A) on bacterial lawns at 22°C, where values represent the mean diameter ± SD of 10 plaques from 1 of 3 representative experiments or (B) in axenic medium at 27°C, where values represent mean ± SD of 3 experiments. (C) Comparison of polysome profiles from *sbdS*$^{int(ts)}$ cells transformed with empty vector control (pDXA-3C) or a plasmid expressing eIF6^{T56K} (pDXA-eIF6^{T56K}). (D) Expression of eIF6^{T56K} suppressor protein or actin control in *sbdS*$^{int(ts)}$ cells, visualized by immunoblotting of cell extracts. (E) SBDS is required for nuclear recycling of eIF6. Subcellular fractionation of wild-type compared with *sbdS*$^{int(ts)}$ cells grown at 22°C or 27°C for 12 hours was performed and the indicated proteins visualized by immunoblotting. Histone H3, nuclear marker. Extracts from "total" and "cytoplasmic" fractions represent 2×10^5 cells; nuclear fraction, 2×10^6 cells. (F) Quantification of eIF6 redistribution in SBDS-depleted cells. Ratios were calculated by densitometry. Cyto indicates cytoplasmic; and Nuc, nuclear. (G) eIF6 cosediments with 60S subunits in SBDS-depleted cells. Extracts from wild type control and *sbdS*$^{int(ts)}$ cells were fractionated by sucrose gradient sedimentation in high-salt (0.5M KCl) buffer and immunoblotted to detect eIF6. The sedimentation positions of 40S, 60S, and 80S ribosomes are indicated. Input (In) represents 1% of loaded lyzate.

in a ribosomal subunit joining defect and the accumulation of pre-60S ribosomes (supplemental Figure 11A-B). These particles are loaded with SBDS-GFP and both eIF6 and EFL1^{FLAG} (detected both by immunoblotting and mass spectrometry; see later for EFL1^{FLAG}), suggesting that the mutant SBDS protein blocks ribosome assembly at an intermediate stage, where all 3 proteins are bound to the pre-60S subunit. We conclude that SBDS is required for efficient ribosome assembly in *Dictyostelium,* and directly or indirectly interacts with eIF6 to allow its efficient recycling.

SBDS and EFL1 interact directly in vivo and cocatalyze eIF6 release

In light of these results, we sought a more biochemical understanding of the role of SBDS in eIF6 cycling, first by testing for physical interactions between the key postulated components, SBDS and the GTPase EFL1. EFL1 was tagged by knocking in an N-terminal $2 \times$ FLAG tag (EFL1^{FLAG}) to give a fully functional fusion protein, which was shown to be cytoplasmic in wild type cells by subcellular fractionation (supplemental Figure 12A-F). Similarly, SBDS was also cytoplasmic, with only a faint trace in the nuclear fraction (supplemental Figure 12G).

Endogenous SBDS clearly coimmunoprecipitated with knocked-in EFL1^{FLAG} but the interaction was much stronger after cross-linking with dithiobis(succinimidylpropionate) (DSP; Figure 4A). Similarly SBDS-GFP coimmunoprecipitated with knocked-in EFL1^{FLAG} and GFP-EFL1 coimmunoprecipitated with endogenous SBDS, but a GFP control failed to coimmunoprecipitate endogenous EFL1^{FLAG} or SBDS (supplemental Figure 13). The SBDS-EFL1^{FLAG} interaction was destroyed by incubating lyzates with ribonuclease before crosslinking and immunoprecipitation, but not afterward, suggesting that their association depends on the presence of ribosomal particles (Figure 4B).

The size of the SBDS/EFL1^{FLAG} complex was determined using a nonreducible crosslinker (DSS; disuccinimidyl suberate), which remains intact during SDS gel electrophoresis (Figure 4C). The molecular weight of the cross-linked species reciprocally immunoprecipitated with anti-SBDS and anti-FLAG antisera was ~ 160 kDa, consistent with a 1:1 stoichiometric complex of the 2 proteins (theoretical MW = 30.6 + 130.1 + 2(FLAG) = 163 kDa). The identity of the cross-linked species was further confirmed by mass spectrometry (data not shown). These data suggest that SBDS and EFL1 are bound in close physical proximity on the surface of the 60S ribosomal subunit, most likely in a 1:1 stoichiometric complex.

Guided by these results, we developed an in vitro assay for eIF6 release, taking advantage of the fact that eIF6 remains bound to pre-60S ribosomal subunits isolated from SBDS-deficient *Dictyostelium* cells (supplemental Figure 14). These pre-60S ribosomal

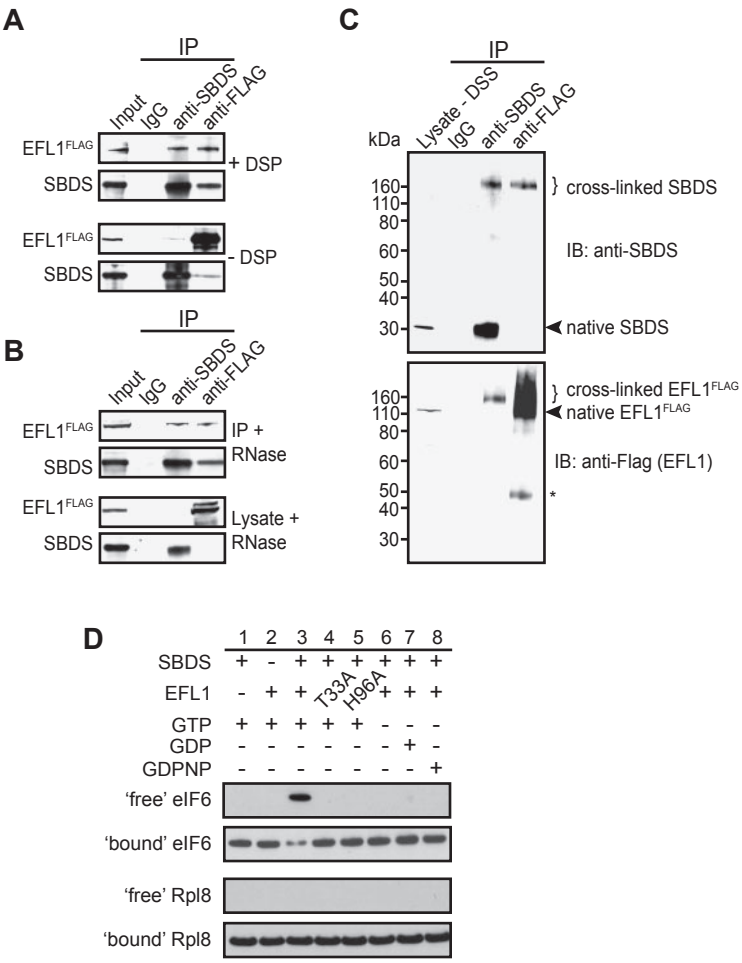

Figure 4. SBDS interacts directly with the GTPase EFL1 to jointly trigger eIF6 eviction. (A) In vivo interaction between endogenous SBDS and EFL1^{FLAG}. Lyzates from *eflA^{FLAG}* cells treated with DSP (+) or vehicle (DMSO) alone (-DSP) were immunoprecipitated with isotype control (IgG), anti-SBDS or anti-FLAG antibodies and the indicated proteins visualized by immunoblotting. Input represents 5% material used for immunoprecipitations. (B) In vivo interaction between endogenous SBDS and EFL1^{FLAG} is RNA-dependent. Lyzates were immunoprecipitated as in panel A after treatment with ribonuclease (RNase) before (bottom) or after (top) incubation with DSP. (C) Direct interaction between SBDS and EFL1^{FLAG} in vivo. Lyzates from *eflA^{FLAG}* cells treated with the crosslinker DSS were immunoprecipitated as in panel A. Native (arrowheads) and crosslinked (brackets) SBDS and EFL1^{FLAG} were visualized by immunoblotting (IB). Cell lysate untreated with DSS (1% of input) was loaded as a control (left). *Indicates mouse IgG heavy chain. (D) Human SBDS and EFL1 jointly catalyze eIF6 release. The indicated combinations of recombinant human SBDS and EFL1 (wild-type or the catalytically inactive mutants EFL1^{T33A} and EFL1^{H96A}) were incubated with pre-60S subunits purified from *sbdS$^{int(ts)}$* cells in the presence of GTP, GDP or the nonhydrolysable analog GDPNP. "Free" and "bound" fractions from sucrose cushions were immunoblotted to detect eIF6 and Rpl8.

subunits are incubated in the release assay, and then sedimented at high *g*-force to separate bound and free eIF6. As human SBDS is functional in *Dictyostelium* cells, human proteins were used in the assay. Figure 4D, lanes 1-3, shows that eIF6 remains associated with *Dictyostelium* pre-60S ribosomal subunits in control incubations, but can be released from them by a combination of human SBDS and EFL1 proteins and GTP, all 3 of which are required. By contrast, 2 catalytically inactive EFL1 mutants (T33A and H96A) were ineffective in catalyzing eIF6 eviction (Figure 4D lanes 4,5) and release did not occur in the absence of GTP, or in the presence of GDP or the nonhydrolysable GTP analog GDPNP (Figure 4D lanes 6-8). There was no detectable dissociation of ribosomal protein Rpl8 during the assay, indicating that there was no general release of ribosomal proteins. Thus, we conclude that SBDS and EFL1 cooperate to directly catalyze the release of eIF6 from pre-60S subunits by a mechanism that requires GTP binding and hydrolysis.

Lymphoblasts from SDS patients exhibit defective ribosomal subunit joining

This work, together with that in yeast[13] and mouse,[7] compellingly demonstrates that SBDS has a conserved role in ribosome assembly. We therefore next sought in vivo evidence for defective subunit joining in SDS patient–derived cells, despite an earlier negative study.[12] The reported B-cell defects in SDS[24] prompted us to analyze polysome profiles from SDS patient–derived B-lymphoblastoid cell lines. Compared with wild type control, sucrose density centrifugation analysis of cell extracts from 3 independent lymphoblastoid cell lines derived from SDS patients carrying *SBDS* mutations revealed clear evidence of defective ribosomal subunit joining (Figure 5A; supplemental Table 4). SBDS protein expression in the SDS lymphoblasts was reduced to between $< 1\%$ and 48% of wild-type levels, and correlated inversely with the severity of the joining defect, whereas the expression of eIF6 and the ribosomal export protein, NMD3 was increased 1.7- to 2.3-fold (Figure 5B). RPL11 and RPL23 expression was unaffected as was that of the assembly factors EFL1 or EBP1 (the mammalian homologue of yeast Arx1).

Discussion

In this study, we have tested the hypothesis that the SBDS protein has a conserved function in 60S subunit maturation and ribosome assembly and that this defect underlies the pathogenesis of SDS. We have combined the analysis of human SDS patient-derived cells and mutant *Dictyostelium* cells carrying temperature-sensitive, self-splicing inteins inserted into the coding sequence of the *Dictyostelium sbdS* gene, allowing for the rapid depletion of functional SBDS protein from cells at the restrictive temperature. Using this approach, we conclude that (1) SBDS is a cytoplasmic protein required for the release and nuclear recycling of eIF6 from late cytoplasmic pre-60S subunits in *Dictyostelium* cells; (2) wild type human SBDS, but not SDS-associated disease variants,

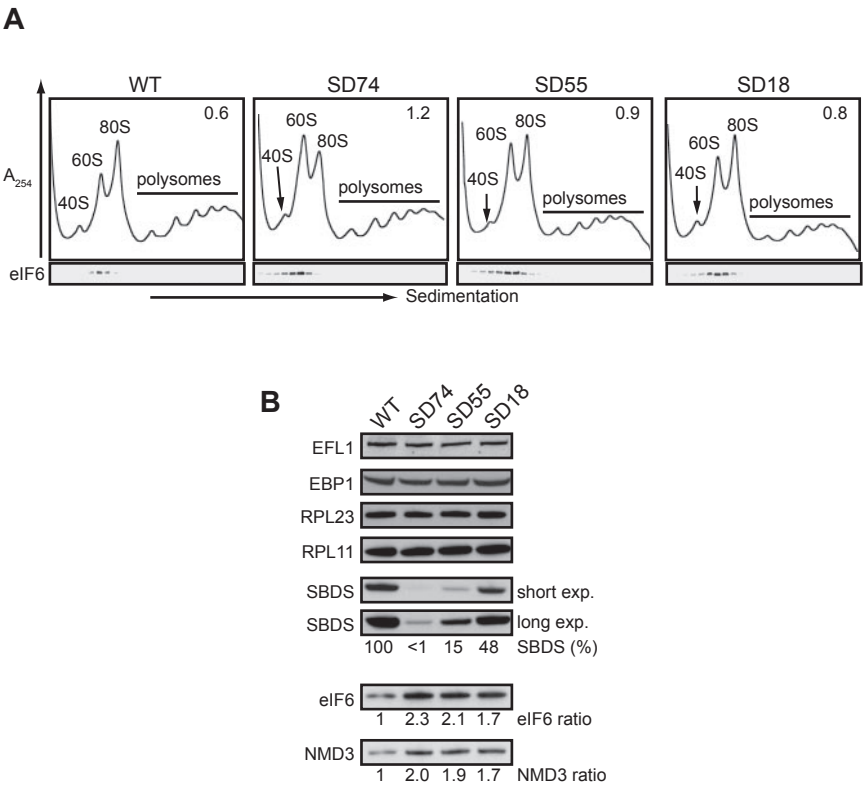

Figure 5. Lymphoblasts from SDS patients exhibit defective ribosome assembly. (A) Comparison of polysome profiles from wild type and SDS patient–derived lymphoblastoid cell lines. Proteins were immunoblotted to visualize eIF6. Ribosomal subunit ratios (605:805) are indicated in the top right corner. *SBDS* genotypes in the patient-derived lymphoblastoid cell lines (SD74, SD55, and SD18) are provided in supplemental Table 4. (B) Extracts from wild type and 3 SDS patient–derived lymphoblastoid cell lines were immunoblotted to visualize the indicated proteins.

genetically complements the growth and ribosome assembly defects in mutant *Dictyostelium* cells; (3) SBDS and the GTPase EFL1 directly interact in vivo on the ribosome; (4) human SBDS and EFL1 cooperate in the presence of GTP to catalyze the eviction of eIF6 from late cytoplasmic pre-60S subunits in *Dictyostelium*. Critically, the ribosome assembly defect that we have demonstrated in lymphoblasts from SDS patients is consistent with the genetic data in *Dictyostelium* (this work), yeast,[13] and murine[7] systems. Thus, there seems little doubt that the fundamental and conserved role of the SBDS protein is to catalyze a late cytoplasmic step in the maturation of the 60S ribosomal subunit and thereby allow the assembly of actively translating ribosomes. Although a ribosome assembly defect was not observed in fibroblasts from an SDS patient,[12] this may simply reflect higher SBDS protein expression or a reduced requirement for SBDS in fibroblasts compared with B-lymphoblastoid cell lines.

Our findings strongly support the hypothesis that SDS is a ribosomopathy caused by impaired release of eIF6 and defective ribosomal subunit joining as a consequence of deficiency of the ribosome assembly factor SBDS. Thus, the mechanism underlying SDS is distinct from autosomal dominant Diamond-Blackfan anemia (DBA), caused by haploinsufficiency for genes encoding structural components of both the large and small ribosomal subunit[25] and the 5q-syndrome, an acquired subtype of MDS that appears to be caused, at least in part, by haploinsufficiency of the *RPS14* gene.[26-28]

The severity of the defect in ribosomal subunit joining in *Dictyostelium* and in human cells correlates with the expression level of the SBDS protein, at least with respect to the disease variants. We therefore suggest that the varied clinical phenotypes may reflect the level of residual SBDS protein expression coupled with critical threshold requirements for SBDS function in meeting translational demands in different tissues at various times during development.

How can we link defective ribosome assembly to the major clinical phenotypes associated with SDS, particularly the bone marrow failure, exocrine pancreatic insufficiency and skeletal abnormalities? Impaired SBDS function might mediate its effect through consequences on global protein translation, through defective translation of critical proteins or potentially by the induction of stress responses. Increasing evidence in several animal models supports a model in which defective ribosome biogenesis causes p53-dependent developmental abnormalities[28-31] mediated by a ribosomal protein-Mdm2 stress signaling pathway.[32] Indeed, p53 protein overexpression has been reported in the bone marrow cells of SDS patients,[33,34] supporting the potential relevance of this pathway to the pathogenesis of the marrow failure in SDS.

Neutrophils, pancreatic acinar cells and the chondrocytes and osteoblasts of the skeletal system are all characterized by high protein secretory capacity. Thus, in SDS, the acinar cells of the pancreas may be more susceptible to defects in ribosome assembly around the time of weaning, a period of dramatic growth and expansion of the exocrine tissue. Endoplasmic reticulum stress has been reported to induce the cartilage pathology associated with metaphyseal chondrodysplasia type Schmid.[35] We hypothesize that activation of this pathway may be relevant to the pathogenesis of the skeletal pathology in SDS. However, further studies are required to fully understand the pathophysiologic mechanisms underlying the clinical features of SDS.

Our data highlight the power of the genetically tractable model organism *Dictyostelium discoideum* to provide novel insight into the pathogenesis of an inherited human disorder associated with bone marrow failure and leukemia predisposition. We note that the slow growth phenotype of *sbdS*$^{int(ts)}$ cells may facilitate genetic screens to identify novel components of the SBDS-EFL1-eIF6 pathway and to discover small molecules that improve SBDS pathway function and that may have therapeutic potential. Finally,

conditional inteins represent a new technology to investigate the function of essential genes in *Dictyostelium*.

Acknowledgments

The authors thank S. Mitchell for *Dictyostelium* SBDS protein purification, the Japanese cDNA project[36] for providing clone VHA344, dictyBase for expression plasmids, N. Perrimon for plasmid pS5ΔH-G4MINT, and J. Rommens for lymphoblastoid cell lines. They thank F. Begum, S. Peak-Chew, and E. Stephens for mass spectrometry, as well as members of A.J.W. and R.R.K. labs for helpful comments and advice.

The Medical Research Council, the Raymond and Beverly Sackler Fund, Leukemia and Lymphoma Research, the Association for International Cancer Research, the Sylvia Aitken Trust, the MDS Foundation, the Leukemia & Lymphoma Society of America, Shwachman-Diamond United Kingdom, Ted's Gang, the Tesni Parry Memorial Fund, and the Cambridge NIHR Biomedical Research Center supported the work.

Authorship

Contribution: C.C.W., D.T., and A.J.W. designed and performed research, analyzed data, and wrote the paper; R.R.K. designed research, analyzed data, and wrote the paper; and N.B. contributed vital new reagents.

Conflict-of-interest disclosure: The authors declare no competing financial interests.

Correspondence: Prof Alan Warren, University of Cambridge, MRC Laboratory of Molecular Biology, Hills Road, Cambridge CB2 0QH, United Kingdom; e-mail: ajw@mrc-lmb.cam.ac.uk.

References

1. Boocock GR, Morrison JA, Popovic M, et al. Mutations in SBDS are associated with Shwachman-Diamond syndrome. *Nat Genet.* 2003;33(1):97-101.
2. Donadieu J, Leblanc T, Bader Meunier B, et al. Analysis of risk factors for myelodysplasias, leukemias and death from infection among patients with congenital neutropenia. Experience of the French Severe Chronic Neutropenia Study Group. *Haematologica.* 2005;90(1):45-53.
3. Zhang S, Shi M, Hui CC, Rommens JM. Loss of the mouse ortholog of the shwachman-diamond syndrome gene (Sbds) results in early embryonic lethality. *Mol Cell Biol.* 2006;26(17):6656-6663.
4. Shammas C, Menne TF, Hilcenko C, et al. Structural and mutational analysis of the SBDS protein family. Insight into the leukemia-associated Shwachman-Diamond Syndrome. *J Biol Chem.* 2005;280(19):19221-19229.
5. Savchenko A, Krogan N, Cort JR, et al. The Shwachman-Bodian-Diamond syndrome protein family is involved in RNA metabolism. *J Biol Chem.* 2005;280(19):19213-19220.
6. Ng CL, Waterman DG, Koonin EV, et al. Conformational flexibility and molecular interactions of an archaeal homologue of the Shwachman-Bodian-Diamond syndrome protein. *BMC Struct Biol.* 2009;9:32.
7. Finch AJ, Hilcenko C, Basse N, et al. Uncoupling of GTP hydrolysis from eIF6 release on the ribosome causes Shwachman-Diamond syndrome. *Genes Dev.* 2011;25(9):917-929.
8. Kuijpers TW, Alders M, Tool AT, Mellink C, Roos D, Hennekam RC. Hematologic abnormalities in Shwachman Diamond syndrome: lack of genotype-phenotype relationship. *Blood.* 2005;106(1):356-361.
9. Stepanovic V, Wessels D, Goldman FD, Geiger J, Soll DR. The chemotaxis defect of Shwachman-Diamond Syndrome leukocytes. *Cell Motil Cytoskeleton.* 2004;57(3):158-174.
10. Austin KM, Gupta ML, Coats SA, et al. Mitotic spindle destabilization and genomic instability in Shwachman-Diamond syndrome. *J Clin Invest.* 2008;118(4):1511-1518.
11. Ball HL, Zhang B, Riches JJ, et al. Shwachman-Bodian Diamond syndrome is a multi-functional protein implicated in cellular stress responses. *Hum Mol Genet.* 2009;18(19):3684-3695.
12. Ganapathi KA, Austin KM, Lee CS, et al. The human Shwachman-Diamond syndrome protein, SBDS, associates with ribosomal RNA. *Blood.* 2007;110(5):1458-1465.
13. Menne TF, Goyenechea B, Sanchez-Puig N, et al. The Shwachman-Bodian-Diamond syndrome protein mediates translational activation of ribosomes in yeast. *Nat Genet.* 2007;39(4):486-495.
14. Basu U, Si K, Warner JR, Maitra U. The Saccharomyces cerevisiae TIF6 gene encoding translation initiation factor 6 is required for 60S ribosomal subunit biogenesis. *Mol Cell Biol.* 2001;21(5):1453-1462.
15. Gartmann M, Blau M, Armache JP, Mielke T, Topf M, Beckmann R. Mechanism of eIF6-mediated inhibition of ribosomal subunit joining. *J Biol Chem.* 2010;285(20):14848-14851.
16. Senger B, Lafontaine DL, Graindorge JS, et al. The nucle(ol)ar Tif6p and Efl1p are required for a late cytoplasmic step of ribosome synthesis. *Mol Cell.* 2001;8(6):1363-1373.
17. Becam AM, Nasr F, Racki WJ, Zagulski M, Herbert CJ. Ria1p (Ynl163c), a protein similar to elongation factors 2, is involved in the biogenesis of the 60S subunit of the ribosome in Saccharomyces cerevisiae. *Mol Genet Genomics.* 2001;266(3):454-462.
18. Johnson AW, Ellis SR. Of blood, bones, and ribosomes: is Swachman-Diamond syndrome a ribosomopathy? *Genes Dev.* 2011;25(9):898-900.
19. Watts DJ, Ashworth JM. Growth of myxameobae of the cellular slime mould Dictyostelium discoideum in axenic culture. *Biochem J.* 1970;119(2):171-174.
20. Kay RR. Cell differentiation in monolayers and the investigation of slime mold morphogens. *Methods Cell Biol.* 1987;28:433-448.
21. Hoeller O, Kay RR. Chemotaxis in the absence of PIP3 gradients. *Curr Biol.* 2007;17(9):813-817.
22. Zeidler MP, Tan C, Bellaiche Y, et al. Temperature-sensitive control of protein activity by conditionally splicing inteins. *Nat Biotechnol.* 2004;22(7):871-876.
23. Alton TH, Lodish HF. Developmental changes in messenger RNAs and protein synthesis in Dictyostelium discoideum. *Dev Biol.* 1977;60(1):180-206.
24. Dror Y, Ginzberg H, Dalal I, et al. Immune function in patients with Shwachman-Diamond syndrome. *Br J Haematol.* 2001;114(3):712-717.
25. Boria I, Garelli E, Gazda HT, et al. The ribosomal basis of Diamond-Blackfan anemia: mutation and database update. *Hum Mutat.* 2010;31(12):1269-1279.
26. Boultwood J, Pellagatti A, Cattan H, et al. Gene expression profiling of CD34+ cells in patients with the 5q-syndrome. *Br J Haematol.* 2007;139(4):578-589.
27. Ebert BL, Pretz J, Bosco J, et al. Identification of RPS14 as a 5q-syndrome gene by RNA interference screen. *Nature.* 2008;451(7176):335-339.
28. Barlow JL, Drynan LF, Hewett DR, et al. A p53-dependent mechanism underlies macrocytic anemia in a mouse model of human 5q-syndrome. *Nat Med.* 2010;16(1):59-66.
29. Jones NC, Lynn ML, Gaudenz K, et al. Prevention of the neurocristopathy Treacher Collins syndrome through inhibition of p53 function. *Nat Med.* 2008;14(2):125-133.
30. McGowan KA, Li JZ, Park CY, et al. Ribosomal mutations cause p53-mediated dark skin and pleiotropic effects. *Nat Genet.* 2008;40(8):963-970.
31. Barlow JL, Drynan LF, Trim NL, Erber WN, Warren AJ, McKenzie AN. New insights into 5q-syndrome as a ribosomopathy. *Cell Cycle.* 2010;9(21):4286-4293.
32. Macias E, Jin A, Deisenroth C, et al. An ARF-independent c-MYC-activated tumor suppression pathway mediated by ribosomal protein-Mdm2 Interaction. *Cancer Cell.* 2010;18(3):231-243.
33. Elghetany MT, Alter BP. p53 protein overexpression in bone marrow biopsies of patients with Shwachman-Diamond syndrome has a prevalence similar to that of patients with refractory anemia. *Arch Pathol Lab Med.* 2002;126(4):452-455.
34. Dror Y. P53 protein overexpression in Shwachman-Diamond syndrome. *Arch Pathol Lab Med.* 2002;126(10):1157-1158, author reply 1158.
35. Rajpar MH, McDermott B, Kung L, et al. Targeted induction of endoplasmic reticulum stress induces cartilage pathology. *PLoS Genet.* 2009;5(10):e1000691.
36. Urushihara H, Morio T, Tanaka Y. The cDNA sequencing project. *Methods Mol Biol.* 2006;346:31-49.